ELSEVIER

Journal of Hazardous Materials B:64 (1999) 295–311

Journal of Hazardous Materials

Thermogravimetric study of thermal decontamination of soils polluted by hexachlorobenzene, 4-chlorobiphenyl, naphthalene, or *n*-decane

Véronique Risoul [a,b], Claire Pichon [a,b], Gwénaëlle Trouvé [a], William A. Peters [c], Patrick Gilot [a,*], Gilles Prado [a]

[a] *Laboratoire Gestion des Risques et Environnement, Ecole Nationale Supérieure de Chimie Mulhouse, Université de Haute-Alsace, 25 rue de Chemnitz, EA 2334, 68200 Mulhouse, France*

[b] *Trédi, Département Recherche, Technopôle de Nancy-Brabois, B.P. 184-54505 Vandoeuvre lès Nancy, France*

[c] *Energy Laboratory and Center for Environmental Health Sciences, Massachusetts Institute of Technology, 77 Massachusetts Avenue, Cambridge, MA 02139, USA*

Received 3 July 1998; revised 13 July 1998; accepted 7 December 1998

Abstract

To determine decontamination behavior as affected by temperature, shallow beds of a clay-rich, a calcerous, and a sedimentary soil, artificially polluted with hexachlorobenzene, 4-chlorobiphenyl, naphthalene, or *n*-decane, were separately heated at 5°C min^{-1} in a thermogravimetric analyzer. Temperatures for deep cleaning of the calcerous and the sedimentary soil increased with increasing boiling point (bp) of the aromatic contaminants, but removal efficiencies still approached 100% well below the bp. Decontamination rates were therefore modelled according to a pollutant evaporation–diffusion transport model. For the calcerous and sedimentary soils, this model reasonably correlated removal of roughly the first 2/3 of the naphthalene, but gave only fair predictions for hexachlorobenzene and 4-chlorobiphenyl. It was necessary to heat the clay soil above the aromatics bp to achieve high decontamination efficiencies. Weight loss data imply that for temperatures from near ambient to as much as 150°C, interactions of each aromatic with the clay soil, or its decomposition products, result in lower net volatilization of the contaminated vs. neat clay. A similar effect was observed in heating calcerous soil polluted with hexachlorobenzene from near ambient to about 140°C. Decontamination mechanisms remain to be

* Corresponding author. Tel.: +33-3-89-32-76-55; fax: +33-3-89-32-76-61; e-mail: p.gilot@univ-mulhouse.fr

PII: S0304-3894(98)00267-2

established, although the higher temperatures needed to remove aromatics from the clay may reflect a more prominent role for surface desorption than evaporation. This would be consistent with our estimates that the clay can accommodate all of the initial pollutant loadings within a single surface monolayer, whereas the calcerous and sedimentary soils cannot.

Keywords: Pollution; Soils; Hydrocarbons; Thermogravimetric analysis; Thermal decontamination

1. Introduction

Thermal treatment is an appealing technology for cleaning soils contaminated by hydrocarbons [1,2]. Soil thermal treatment methods can be categorized according to their oxygen potential and range of operating temperatures: vitrification under reducing conditions at elevated temperatures (>2000°C) [3]; incineration involving reducing regions followed by oxidation at 1000–1300°C [4]; and thermal stripping at temperatures generally <500°C, and typically involving air or steam as sweep gases to remove volatile or semivolatile organic contaminants for subsequent treatment, e.g., rotary kilns [5–12], thermal augers [9,10,13], fluidized beds [9,14,15], plasma arcs [16], vitrification furnaces [3], and resonant technologies [17].

Laboratory and critical subscale experiments, e.g. Refs. [17–23], as well as mathematical modelling, e.g. Refs. [20,21,23], can provide useful information to help in the selection of soil remediation strategies, and in the design, operation, monitoring and control of specific cleanup technologies. Of particular interest are how operating parameters such as temperature, heating rate, treatment time, flow rate of ambient gas, soil type, and contaminant properties, affect rates and extents of pollutant removal as well as yields and identities of by-products.

Thermogravimetric analysis (TGA) has become a popular technique for studying physical or chemical processes that involve a mass change in a solid [24,25]. This methodology allows use of small samples for which temperature can be reasonably well controlled, and continuous determination of mass gain or loss, with high sensitivity. This paper presents TGA data on the rates and extents of removal of four different organic contaminants spanning a range of volatility, from three different soil types. Characteristic temperature ranges where most of the decontamination occurred, as well as temperatures for maximum rates of decontamination were determined for 11 different soil/pollutant combinations. Insights on physical and chemical processes contributing to the decontamination behavior are deduced from the successes and deficiencies of a pollutant evaporation–diffusion transport model [25] in describing the observed decontamination behavior, and from estimates of the number of pollutant monolayers initially covering each soil.

2. Experimental

2.1. Materials

The soils were three standard European soil samples, supplied by the Environmental Institute (Joint Research Centre, European Commission) at Ispra, Italy: a clay-rich soil,

S_1, (about 75% clays); a mainly calcerous soil, S_2 (about 60% $CaCO_3$) and a sedimentary soil, S_3, (75.5% silt). More detailed descriptions of these soils are given elsewhere [26,27].

2.2. Apparatus

All these contaminated soil samples were subjected to TGA, using a thermobalance CAHN 121. The initial sample mass of about 15 mg was placed in an approximately hemispherical crucible (4 mm deep and 9 mm in cross-sectional diameter at its mouth). The thermobalance operated under a carrier gas flow of nitrogen of 83 $cm^3\ min^{-1}$ (standard conditions) and a heating rate of 5°C min^{-1}. Each experiment was performed 2 or 3 times. Uncontaminated (neat) samples were also subjected to the same temperature–time history to account for removal of volatiles from soil itself.

2.3. Experimental procedure

These soils were artificially and separately contaminated with *n*-decane, hexachlorobenzene (HCB), naphthalene and 4-chlorobiphenyl (4-CBP). The following procedure [28,29] was used. Before being contaminated, the soil samples were crushed and sieved to obtain the 0–400 μm size fraction. A known amount of contaminant (preselected in order to obtain a theoretical pollution level of 4 wt.%) was dissolved in about 200 cm^3 of an appropriate solvent (see Table 1, in which the melting and boiling points of each contaminant are also noted). About 5 g of soil was exposed to the solution of contaminant for 1 h, at a temperature in the range 0–10°C, in a rotating vessel (rotation rate: 50 rpm). After evaporation of the solvent, the soil–contaminant mixture was dried for 12 h at ambient conditions. Then, the contaminated soil sample was kept in a brown pill box, in a refrigerator at about 4°C. The theoretical contamination level, based on uncontaminated soil, was calculated for each soil/contaminant system (see Table 2), by assuming all of the dissolved contaminant was transferred to the soil upon evaporation of the solvent. However, for our determination of soil decontamination a more reliable value of the initial contamination level, derived as described below, was used.

Table 1
Contaminant characteristics and solvents used for the soil contaminations

Contaminant	Molecular weight ($g\ mol^{-1}$)	Melting point (°C)	Boiling point (°C)	Projected surface area of one molecule of contaminant (m^2)	Solvent used for contamination of soils
n-Decane	142.0	−30.0	174.0	3.51×10^{-19}	Dichloromethane
Naphthalene	128.0	80.3	217.9	3.35×10^{-19}	Dichloromethane
HCB	284.8	228.0	324.0	2.46×10^{-19}	Chloroform
4-CBP	188.7	77.7	291.0	4.26×10^{-19}	Diethyl ether

Table 2
Theoretical initial contamination levels, and initial contamination levels measured by TGA (enclosed in parentheses). The values are given in % by weight of uncontaminated soil

Pollutant	Theoretical and measured contamination level for S_1	Theoretical and measured contamination level for S_2	Theoretical and measured contamination level for S_3
Naphthalene	4.2 (2.4)	4.2 (3.2)	4.0 (2.6)
HCB	4.0 (2.5)	4.0 (3.6)	4.8 (4.5)
4-CBP	4.0 (2.9)	3.9 (3.5)	4.0 (3.5)
n-Decane	4.8 (1.5)	4.0 (0.0)	4.0 (0.7)

2.4. Calculations

From these thermogravimetric measurements, the total weight losses of contaminated soils (WL_{CT} in % by weight) and uncontaminated soils (WL_{NCT} in % by weight) were determined.

From thermograms, it appeared that the decontamination process was finished at 450°C. Then WL_{CT} and WL_{NCT} were recorded at this temperature (the neat soil weight loss occurs up to 1000°C). Using WL_{CT} and WL_{NCT}, it was then possible to estimate the initial contamination level CL (% by weight of uncontaminated soil) of the soil by the Eq. (1):

$$CL = \left(\frac{WL_{CT} - WL_{NCT}}{100 - WL_{CT}} \right) 100 \quad (1)$$

Studies of S_1, S_2 and S_3 contaminated with PAH, found that the initial contamination level CL, measured by this TGA method agreed well with the CL determined by extraction of untreated soil followed by GC analysis of PAH in the extract.

From the continuous records of the weight losses of contaminated soils and uncontaminated soils, i.e. the thermograms, it was possible to obtain the decontamination level $DL_{(t)}$, as a function of the time t, throughout the decontamination process [30,31]. The quantity $DL_{(t)}$ is defined as the percentage of the initial mass of contaminant released up to a time t.

3. Mathematical modelling

Contaminant removal from the soil during heat-up with the thermobalance was modelled as evaporation from a liquid phase (or sublimation from a solid phase) uniformly distributed over the particle surface area. The model assumes that mass and heat transfer resistances within the soil particles are negligible. After separation from a soil particle, contaminant removal proceeds by non-reactive diffusive transport through the soil pile and then through a non-reactive concentration boundary layer above the soil surface within the crucible. This model, described in more detail elsewhere [30],

represents the geometric arrangement of the soil and crucible by cylinders of cross-sectional area $S_p = 3.00 \times 10^{-5}$ m^2 and $S_c = 6.36 \times 10^{-5}$ m^2, respectively.

In this model, the rate of evaporation of the contaminant r_p is assumed to be proportional to the difference in the mole fraction of contaminant vapor at the surface of the particle (x_{sat}) and the local mole fraction of contaminant vapor (x) in the gas phase surrounding the particle, according to Eq. (2) [21]:

$$r_p = \frac{12\,DC(x_{sat} - x)}{d_p^2} \tag{2}$$

where D is the molecular diffusivity of the contaminant in the gas phase surrounding the particle, C is the gas concentration and d_p is the diameter of the soil particle ($d_p = 75$ μm). The mole fraction x_{sat} is calculated by assuming thermodynamic equilibrium between contaminant in the vapor phase at the soil surface and contaminant in the condensed phase, i.e., liquid or solid, on the soil surface.

The molecular diffusivities of the contaminant vapor are assumed to vary with temperature T according to Eq. (3):

$$D = aT^{1.5}. \tag{3}$$

The values of a are given in Table 3. The equivalent diffusivity D_e of the contaminant within the soil bed is given by Eq. (4):

$$D_e = \frac{D\varepsilon}{\tau} \tag{4}$$

where ε and τ are the porosity and the tortuosity of the soil bed. These values were taken equal to 0.35 and 4, respectively, whatever the soil. The porosity of 0.35 corresponds to a non-compact staking of particles. It was checked that a tortuosity between 2 and 8 did not significantly change the results obtained with the model. It was established that contaminants are transported through the soil pile to the bed surface by ordinary Fickian diffusion.

The thickness δ of the contaminant concentration boundary layer was estimated for each contaminant, by a separate model of isothermal evaporation of the pure contaminant. This estimation was done at a mean temperature in agreement with the temperature range of decontamination of the given soil/contaminant system. The detailed determination of these different thicknesses is provided elsewhere [25,31]. The relevant value of δ is given with each figure displaying results obtained with the model.

This model is expected to apply only if evaporation of the contaminant is the main mechanism for the contaminant release from each contaminated soil particle. For that

Table 3
Coefficients for estimation of the pollutant diffusivity[a]

Pollutant	Naphthalene	HCB	4-CBP	*n*-Decane
a (m^2 s^{-1} K$^{-1.5}$)	1.3030×10^{-9}	1.5999×10^{-9}	1.0603×10^{-9}	1.1150×10^{-9}

[a] See Eq. (3).

reason, this model was used to predict the release of the contaminant molecules not directly adsorbed onto the soil particle surface. The first monolayer of contaminant molecules, covering the soil surface, is expected to be strongly bound to the soil particles. The fraction f of the contaminant molecules comprising the first monolayer adsorbed on the surface of the soil particle was estimated from the BET surface area S_{BET} of the noncontaminated soil (50.1×10^3 m^2 kg^{-1} for S_1, 8.7×10^3 m^2 kg^{-1} for S_2 and 11.8×10^3 m^2 kg^{-1} for S_3) and the projected surface area S_{mol} of the contaminant molecule (given in Table 1), using the following Eq. (5):

$$f = \frac{100 M S_{BET}}{N_a \times CL \times S_{mol}} \quad (5)$$

where M is the molecular weight of the contaminant (kg mol^{-1}) and N_a is Avogadro's number (mol^{-1}).

Because the decontamination proceeded sequentially down the soil layers within the crucible [30], during the model calculations, the local release of the contaminant from the soil particles had to be stopped when only one monolayer of contaminants remained adsorbed onto the surface of the soil particles situated between two adjacent computational grid points within the soil bed. This was done, locally, when the residual contamination level CL'_{res} (in % by weight of contaminated soil) corresponding to coverage of the soil by just one monolayer of contaminant was reached within the soil bed during the computation. The value of CL'_{res} was calculated by Eq. (6):

$$CL'_{res} = \frac{100 f \times CL}{100 + CL}. \quad (6)$$

The values of f and CL'_{res} are given in Table 4 for each system soil/contaminant, together with the initial mass of the contaminated soil used in the simulation and in the

Table 4
Experimental and model inputs for the different soil/contaminant systems

Soil/ contaminant system	Initial mass of contaminated soil (mg)	Real contamination level (% weight of uncontaminated soil)	f[a]	n[b]	CL'_{res}[c] (% weight of contaminated soil)
S_1/HCB	14.300	2.5	1	1	2.4
S_1/4-CBP	14.444	2.9	1	1	2.8
S_1/naphthalene	14.518	2.4	1	1	2.3
S_1/*n*-decane	14.622	1.5	1	1	1.5
S_2/HCB	14.690	3.6	0.46	< 3	1.6
S_2/4-CBP	14.913	3.5	0.18	< 6	0.6
S_2/naphthalene	14.468	3.2	0.17	< 6	0.5
S_3/HCB	14.578	4.5	0.50	2	2.2
S_3/4-CBP	14.455	3.5	0.25	4	0.8
S_3/naphthalene	14.312	2.6	0.29	< 4	0.7

[a] Fraction of real contaminant loading calculated to be in the first monolayer covering the soil BET surface area (see text).
[b] Total number of monolayers to hold the entire initial loading of contaminant.
[c] The calculated amount of contaminant needed to just cover the soil BET surface area with one monolayer.

experiment. For example, line 5 of Table 4, (S_2/HCB) means that the model predicts 54% of decontamination, $100(1-f)$, leading to a residual contamination level of 1.6% by weight of contaminated soil.

The operating pressure was 10^5 Pa. A finite difference method was used with 60 mesh nodes in the soil and 10 mesh nodes in the concentration boundary layer. The temperature step was 0.1 K.

4. Results

Table 2 compares the theoretical contamination levels (CL) to the initial contamination levels measured by TGA, for the different systems soil/contaminant. The measured contamination levels are much less than the theoretical ones of about 4%. It was not possible to contaminate the soil S_2 by *n*-decane and the soil S_3 was only slightly contaminated by this contaminant. These low values for the observed initial contamination are due to the fact that much of the contaminant is vaporized during the solvent evaporation step. This phenomenon is particularly evident when *n*-decane, a compound of high volatility, was used. The soils S_1 and S_2 were contaminated to an extent of about 2.5–3% and 3–3.5%, respectively, except when *n*-decane was the contaminant. The contamination level of the soil S_3 was much more affected by the nature of the contaminant. The chlorinated compounds (HCB and 4-CBP) seem to have been more retained by the soils, particularly the soil S_3.

In Fig. 1, four curves show the decontamination level (%) as a function of temperature, for the soil S_1 separately contaminated by naphthalene, HCB, 4-CBP and *n*-decane. Most of the contaminant is released well before its boiling point and

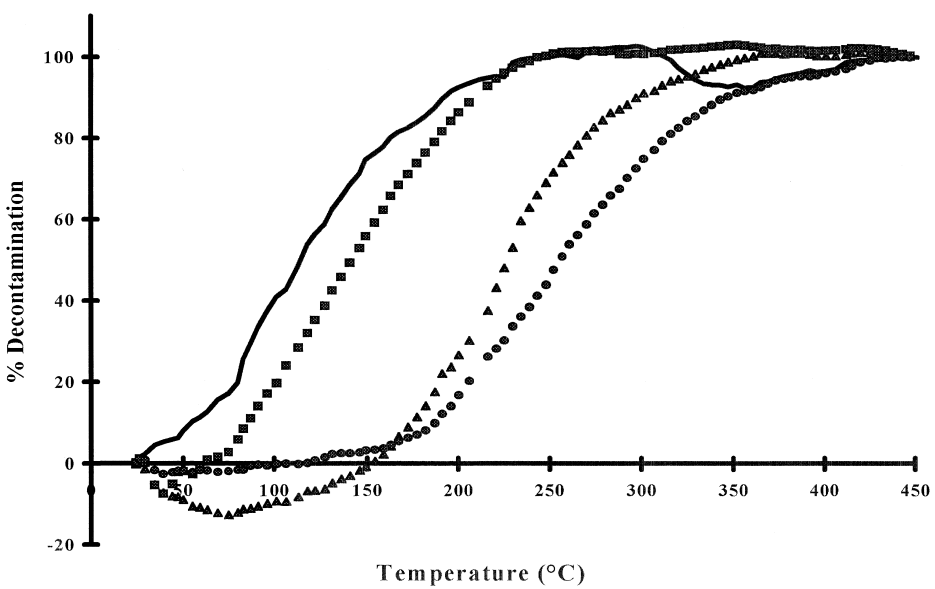

Fig. 1. Decontamination level as a function of temperature for the soil S_1 contaminated by 4-CBP ▲, HCB ●, naphthalene ■, *n*-decane ————. Heating rate 5°C min^{-1}.

decontamination approaches completion at about 250°C for *n*-decane and naphthalene, 350°C for 4-CBP and 450°C for HCB. The end of the decontamination cannot be studied with enough accuracy using this TGA, owing to the very small changes in the sample mass with increasing temperature as contaminant removal approaches completion. For a given soil, the order in which contaminants are released is the same as their boiling points, the *n*-decane with the lower boiling point being removed over the lower temperature range. This is very clear in Fig. 1 for S_1 and is also the case for the two other soils.

Figs. 2–4 show the decontamination level (%) for the different soils as a function of temperature for the contaminants 4-CBP, HCB, and naphthalene, respectively. The decontamination curves (Figs. 1–4) are constructed by assuming that throughout the heating protocol, the presence and release of the pollutant does not affect weight loss of the soil, and vice versa. The presents results imply that this assumption breaks down for some ranges of temperature and certain soil/contaminant combinations. For all three aromatic pollutants, the clay soil (S_1) shows negative extents of decontamination at temperatures from near ambient up to 60–150°C (Fig. 1). Similar behaviour was observed from near ambient to about 140°C in removing hexachlorobenzene from the calcerous soil (S_2) (Fig. 3). These effects suggest that contaminants interact with the soil itself or with soil-derived volatiles so that soil in the presence of contaminant undergoes lower net weight loss than neat soil over the stated temperature ranges. Because of the relatively low temperatures, and the attainment of virtually 100% contaminant removal at higher temperatures, it seems unlikely that coking of some of the contaminant on the soil surface is responsible.

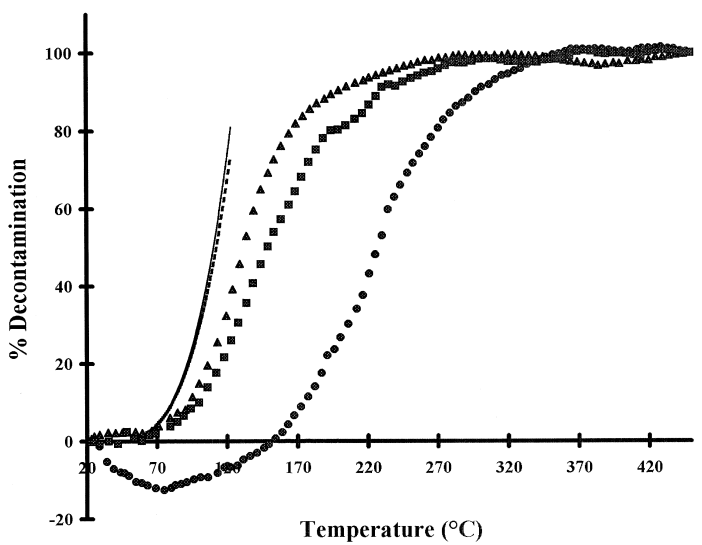

Fig. 2. Decontamination level as a function of temperature for 4-CBP. Heating rate 5°C min^{-1}. $\delta = 4.6$ mm. ———— soil S_2 model; --- soil S_3 model; ● soil S_1 experiment; ▲ soil S_2 experiment; ■ soil S_3 experiment.

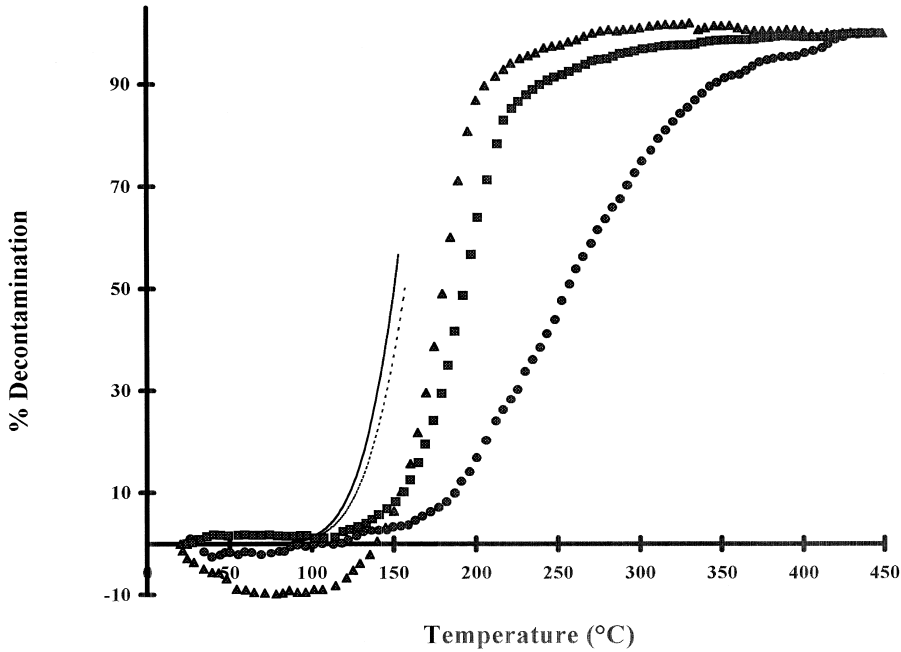

Fig. 3. Decontamination level as a function of temperature for HCB. Heating rate 5°C min^{-1}. $\delta = 5.6$ mm. ———— soil S_2 model; --- soil S_3 model; ● soil S_1 experiment; ▲ soil S_2 experiment; ■ soil S_3 experiment.

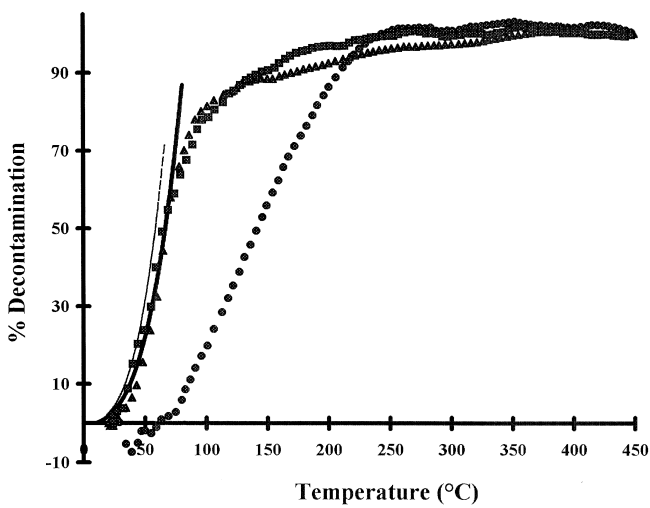

Fig. 4. Decontamination level as a function of temperature for naphthalene. Heating rate 5°C min^{-1}. $\delta = 5.5$ mm. ———— soil S_2 model; --- soil S_3 model; ● soil S_1 experiment; ▲ soil S_2 experiment; ■ soil S_3 experiment.

In order to better characterize the release of the contaminant, two temperature ranges of decontamination were defined. The instantaneous decontamination rate (v in mg s^{-1}) was chosen as one index of decontamination intensity.

This rate, a function of time (with m_{co} the initial contaminant mass), defined by the Eq. (7):

$$v(t) = \frac{m_{co}}{100} \frac{d[DL(t)]}{dt} \tag{7}$$

rises to its maximum v_{max} at a temperature T_{max} and then decreases. The first temperature range R_1 corresponds to a decontamination rate higher than one tenth of the maximum rate. The second range of temperatures R_2 corresponds to a decontamination rate exceeding one half the maximum rate. The first range is rather characteristic of the 'total' decontamination process while the second range characterizes the fast part of the decontamination process.

These temperature ranges R_1 and R_2 are shown in Fig. 5 for the different decontamination experiments carried out under atmospheric pressure. In this figure, the melting and boiling points of each contaminant are also indicated, for comparison with R_1 and R_2. The values of T_{max} and v_{max} obtained during these experiments are presented in Fig. 6.

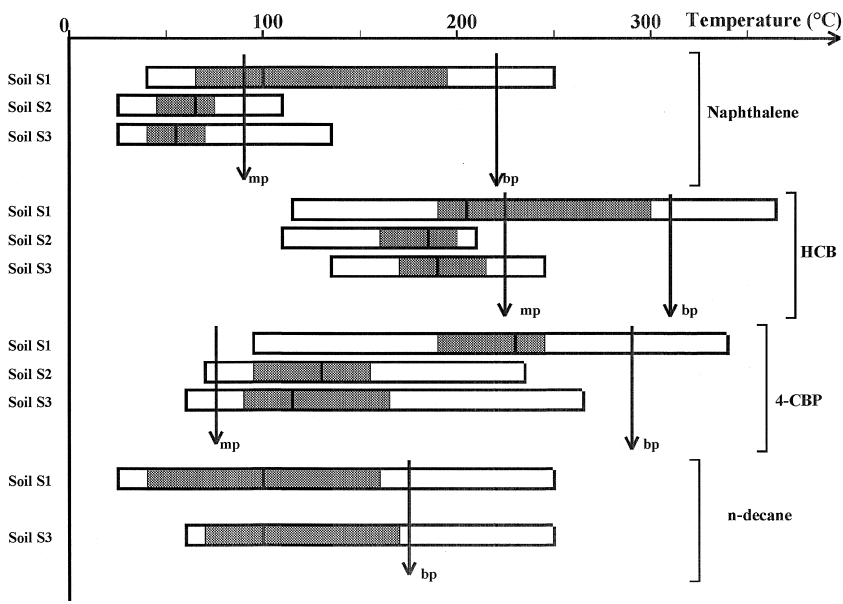

Fig. 5. Temperature ranges of decontamination for three different soils separately contaminated by four organic compounds. Heating rate 5°C min^{-1}. □: $v > 0.1v_{max}$ and ■: $v > 0.5v_{max}$; | : Temperature corresponding to the maximum rate of decontamination. mp: melting point; bp: boiling point, v = decontamination rate in mg s^{-1}, see text and Eq. (4).

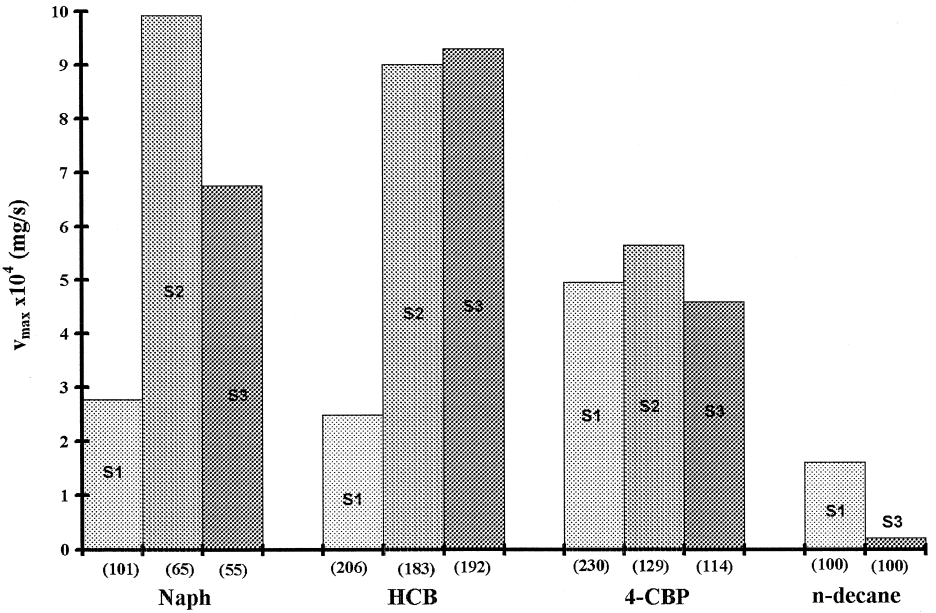

Fig. 6. Maximum observed decontamination rates and corresponding temperatures for several soil/pollutant combinations. Heating rate 5°C min^{-1}. The temperatures are indicated between brackets.

Although the temperatures T_{max} are different, all the maximum decontamination rates v_{max} are roughly of the same order of magnitude, except for the decane/S_3 system. Moreover, they are very similar for all three soils for 4-CBP. The maximum rates corresponding to the soil S_1 contaminated by naphthalene or HCB are 2 to almost 4 times smaller than the corresponding rates for the soils S_2 and S_3. Except for the case of the *n*-decane, the temperatures T_{max} corresponding to a given contaminant are always higher for the clay soil S_1. Whatever the soil/pollutant system, T_{max} is always much lower than the boiling point of the pure contaminant (Fig. 5).

Regarding the different temperature ranges R_1 (Fig. 5), the soil S_1 always exhibits a wider range whatever the contaminant. The same observation prevails for the temperature ranges R_2, except when the soil S_1 was contaminated by 4-CBP. The soil S_1 is the only soil which necessitates a temperature higher than the boiling point of the contaminant to achieve essentially complete removal of the naphthalene, HCB and 4-CBP pollutants. The soils S_2 and S_3 contaminated by naphthalene and HCB, contaminants which sublime, undergo most of their decontamination below the melting points of these contaminants, and the decontamination is completed well below their boiling points. The same soils, S_2 and S_3, polluted by *n*-decane or 4-CBP, begin significant decontamination, i.e. first exceed rates of $0.1v_{max}$, very near the melting point for 4-CBP and at ambient temperature for *n*-decane (data not shown here for S_2). In the case of *n*-decane contaminating the soils S_1 and S_3, it is necessary to heat the soil above the boiling point of *n*-decane to complete decontamination.

5. Discussion

Compared to the calcerous and sedimentary soils (S_2 and S_3), the clay-rich soil S_1 exhibits different decontamination behavior, i.e. for naphthalene, 4-CBP, and HCB a broader range of temperatures for decontamination, and a higher final temperature for contaminant elimination. We assume that each pollutant is uniformly distributed over all the accessible surface area of each soil, and that differences in soil–contaminant interactions contribute to differences in the thermal release of pollutants from the soil. For S_1, the BET surface area is so high that even at the highest contamination levels, each pollutant is calculated to cover less than one monolayer of this soil (Table 4). Consequently we infer that the vapor pressure of each contaminant above the surface of this soil is determined by equilibrium between pollutant vapor and an adsorbed phase on this soil. This adsorbed phase may reflect significant soil–pollutant binding energy [32,33] leading to an equilibrium vapor pressure of contaminant considerably less than that from equilibrium with pure liquid or solid, at the same temperature. Consequently x_{sat} is reduced leading to a lower driving force for contaminant separation from the soil particle (Eq. (2)). Thus the overall rate of decontamination is slower and a higher temperature is needed for achieving high levels of contaminant removal (Fig. 1).

The organic fraction contents of S_1, S_2 and S_3 are 2.65, 6.4, and 2.35 wt.%, respectively. Thus we infer that for all three soils, most of the surface area is provided by the minerals. For S_1 approximately 65% of these minerals are clay-like. Thus we propose that for S_1, the pollutants are primarily adsorbed on clay-like structures and thus it is these structures that provide the strong binding of these pollutants. This proposition assumes that the organic and inorganic sites are equally physically accessible to the contaminants, and that the organic sites do not preferentially bind, e.g. owing to dissolution, the contaminants. We view the latter as improbable because the inventory of organic sites does not dramatically exceed the initial pollutant loadings.

Despite its relatively small abundance, the soil organic matter suggests a plausible explanation for one of the current observations for S_1 and S_2. Negative weight losses were observed for S_1 with any of the four pollutants (Fig. 1) and with S_2 + HCB (Fig. 3). The neat soils specimens were dried in an oven at 50°C for 2 days before being contaminated. Thus it seems unlikely that any of the exogenous pollutant would be partitioned into residual physical moisture in the soil [34,35]. Similarly it seems unlikely that the negative weight loss could be explained by a missing contribution of physical moisture evaporation to low temperature weight loss (for polluted soils). The negative weight losses occurred at lower temperatures where for dried neat soil, weight loss presumably originates from decomposition of soil organic constituents rather than from soil minerals. Consequently, we infer that for the stated combinations of soil and contaminant, one plausible explanation for the negative weight loss is that the exogenous pollutant interferes with release of volatiles from soil organic matter. Another possibility is that during contamination the solvent alters the soil organic or mineral constituents.

For soils S_2 and S_3, with a low BET surface area, only a fraction of the contaminant is expected to be strongly bound to the soil surface, i.e. in the first layer of coverage. This is particularly true for the soils S_2 and S_3 contaminated by 4-CBP and naphthalene (Table 4). Then, from 3–4, to 6 monolayers of molecules are superimposed over the soil

surface and most of the contaminant is only loosely bound and expected to be released from the particles by evaporation. Only the last molecular layer has to desorb directly from the surface of the particles and requires a higher temperature. This hypothesis of evaporation partly controlling the release of the contaminant for the soils S_2 and S_3 is in agreement with the fact that the ranges R_1 and R_2 are shifted towards high temperatures when the boiling points of the contaminants increase, e.g. in Fig. 5, compare S_2/naphthalene and S_3/naphthalene with S_2/HCB and S_3/HCB, and with S_2/4-CBP and S_3/4-CBP. The BET surface areas for the present soils may overestimate the amount of surface area available to the four pollutant molecules. This would be so if some of the soil surface accessible to the standard BET gases (N_2 and CO_2) is inaccessible to contaminants of larger cross-sectional area. Thus the number of monolayers needed to accommodate to entire initial loading of contaminants on the three soils may be larger than those estimated in Table 4 (as the quantity n).

This could in turn mean that evaporation (sublimation) rather than desorption from the soil surface would be responsible for removal of a greater fraction of the contaminant.

The model can be used to support the proposition that evaporation controls the decontamination process of soils S_2 and S_3. Figs. 2–4 illustrate the ability of the model to describe removal of the contaminants 4-CBP, HCB and naphthalene from the different soils. The decontamination curves predicted by the model are almost independent of the nature of the soil, for a given contaminant. The reason is that the model parameters representing the different soil media (porosity, tortuosity, geometry of the soil pile) are the same as are the initial soil masses. The only differences in the model arising from soil type are the residual contamination levels depending on the BET surface area of the soil and the initial contamination level of the soil. These two differences have only a small effect on the rate of contaminant release. In Figs. 2–4, the experimental curves obtained for S_1 are given for comparison.

For soils S_2 and S_4 the range of naphthalene decontamination expected to be controlled by evaporation/sublimation–diffusion is 0–83% and 0–71%, respectively (Table 4). The agreement between the model predictions and the experimental data is quite good over most of these decontamination ranges (Fig. 4).

Agreement is not good for the other contaminants (4-CBP and HCB). For 4-CBP (Fig. 2), the predicted temperatures, at which a given extent of decontamination of 50% is reached, are 22°C and 38°C too low for S_2 and S_3, respectively. For HCB (Fig. 3), these temperatures are 30°C and 35°C too low for S_2 and S_3, respectively. For 4-CBP and HCB the shift between the predicted temperature and the experimental temperature, for a given extent of decontamination, increases with the temperature, for both soils S_2 and S_3. The relative insensitivity of the model to parameters such as mean soil particle diameter, soil bed porosity, soil bed tortuosity and the areas S_c and S_p, shows that uncertainties about these parameters cannot explain the absence of good agreement. The only model parameter having a significant effect is the boundary layer thickness. Thus, for the system S_3/4-CBP (Fig. 2), a decrease of the thickness of the concentration boundary layer from 4.6 to 2.0 mm decreases by 18°C the predicted temperature to achieve 50% decontamination. Since the thicknesses used were previously validated by modelling evaporation of the pure contaminants under the same heating rate, using the

same geometric parameters, uncertainties about this particular parameter are not believed to be responsible for the observed differences [25].

The lack of agreement between the experimental data and data predicted by the model could be due to stronger interactions between the molecules of contaminant themselves, than those accounted for in the model of evaporation. Probably, interactions between contaminant molecules, even those which do not belong to the first layer covering the surface, and the soil itself, are at work, demanding higher temperatures for decontamination. Another reason could be that the molecules of contaminant are situated within the micropores of the soil. For example, bentonite, a swelling clay, can adsorb organic molecules in an 'interfoliaceous' space of 1.4 nm, leading to a high temperature range R_1 for decontamination. The behavior of the soil S_1 can be attributed to the presence of 11.3% of smectite, another swelling clay, comparable to bentonite. Kaolinite although present at a level of 41% in S_1 seems not to be responsible for the unusual behaviour of S_1. The soil S_2 contains a lower amount of smectite (6.8%) but this could still play an important role in the contamination and decontamination processes.

A model based on evaporation (sublimation)–diffusion provides an upper bound on how fast a contaminant can be released from the soil. The good agreement obtained with naphthalene, in the case of the soils S_2 and S_3, shows that for a contaminant of high volatility, evaporation (sublimation)–diffusion is a plausible mechanism when the soil does not exhibit a high microporosity.

6. Conclusions

Important details of the thermal removal of organic contaminants from soil can be deduced from TGA experiments. At a fixed heating rate, temperature ranges to initiate significant decontamination, to achieve maximum rates of decontamination, and to bring decontamination virtually to completion, can be determined by comparing thermograms for neat (uncontaminated) soil and the polluted soil. These comparisons assume that contaminant interactions with soil and its decomposition products during heating are either negligible, or that their effects on soil weight loss can be corrected for. The current work finds evidence of such interactions at low temperatures, i.e., from near ambient to as much as 150°C for a clay-rich soil and three aromatic pollutants (naphthalene, hexachlorobenzene, and 4-chlorobiphenyl) and for a calcerous soil and hexachlorobenzene from near ambient to about 140°C. Temperatures for deep cleaning of the calcerous and a sedimentary soil increased with increasing boiling point (bp) for each aromatic contaminant, but removal efficiencies still approached 100% well below the bp. To achieve high decontamination efficiencies for the clay soil, it was necessary to heat well above the contaminant boiling point for all three aromatics and for *n*-decane. A plausible explanation is that thermal decontamination more closely approximates: (a) evaporation when much of the pollutant is held in multiple monolayers; but (b) desorption from a surface when most of the pollutant is confined to a single surface monolayer. We estimate that the calcerous and sedimentary soils hold from 50% to $>80\%$ of the three aromatic contaminants above the first monolayer, whereas the clay soil hosts all four contaminants within the first monolayer. Thus when soil contamina-

tion levels exceed monolayer coverages, modelling decontamination rates in terms of pollutant evaporation becomes of interest. Here, agreements between experiment and predictions of a contaminant evaporation–diffusion transport model from Pichon et al. [25] varied with contaminant type and soil type, but were most satisfying for a soil/pollutant combination with the highest estimated initial number of monolayer coverages, i.e., the calcerous soil with naphthalene. This model could be improved by accounting for intraparticle transport of contaminants and for soil–contaminant interactions.

7. Nomenclature

a	coefficient for the calculation of D ($m^2\ s^{-1}\ K^{-1.5}$)
C	contaminant gas phase concentration (mol m^{-3})
CL	contamination level of the soil (wt.% of uncontaminated soil)
CL'_{res}	residual contamination level (wt.% of contaminated soil)
D	molecular diffusivity of contaminant in the gas phase surrounding the soil ($m^2\ s^{-1}$)
D_e	effective diffusivity of contaminant within the soil bed ($m^2\ s^{-1}$)
$DL_{(t)}$	cumulative decontamination level of the soil up to time t (wt.% of initial contaminant removed)
d_p	soil particle diameter (m)
f	fraction of the contaminant molecules comprising the first monolayer adsorbed on the surface on the soil particle
M	molecular weight of contaminant (kg mol^{-1})
m_{co}	mass of contaminant at time 0 (kg)
N_a	Avogadro's number (mol^{-1})
P	pressure (Pa)
r_p	evaporation rate (per unit of volume of particles) (mol $m^{-3}\ s^{-1}$)
S_{mol}	contaminant molecule area (m^2)
S_{BET}	BET surface area of uncontaminated soil ($m^2\ kg^{-1}$)
S_c	cross-sectional area of the crucible (m^2)
S_p	cross-sectional area of the soil pile (m^2)
t	time (s)
T	temperature (K)
v	instantaneous decontamination rate (mg s^{-1})
WL_{CT}	weight loss of contaminated soil (%)
WL_{NCT}	weight loss of uncontaminated soil (%)
x	mole fraction of contaminant in the vapor phase
x_{sat}	mole fraction of contaminant in the vapor phase at the surface of the soil particle
δ	thickness of the contaminant concentration boundary layer (m)
ε	soil bed porosity (dimensionless)
τ	soil bed tortuosity (dimensionless)

Acknowledgements

We thank TREDI and the French 'Ministère de l'Industrie' for financial support of this project. We thank the Environmental Institute of 'The Joint Research center, European Commission', at Ispra, Italy, for providing us standard European soil samples. We also thank Drs. LeDred and Kessler for providing us samples of bentonite and kaolinite. Financial support of research at MIT on soil decontamination by NIEHS Grant No. ESO4675 (MIT-Superfund Hazardous Substances Basic Research Program), is also gratefully acknowledged. We thank two reviewers for pointing out alternative explanations for negative weight loss at low temperature.

References

[1] W.W. Kovalik, J. Kingscott, in: W.J. Van den Brick, R. Bosman, F. Arendt (Eds.), Contaminated Soil '95, Kluwer Academic Publishers, London, 1995, pp. 29–38.
[2] R.C. Reintjes, C. Schuler Jr., in: W.J. Van den Brick, R. Bosman, F. Arendt (Eds.), Contaminated Soil '95, Kluwer Academic Publishers Publishers, Netherlands, 1990, pp. 885–894.
[3] A.P. Jackmann, R.L. Powell, in: Hazardous Waste Treatment Technologies, Biological Treatment, Wet Air Oxidation, Chemical Fixation, Chemical Oxidation, Noyes Publications, USA, 1990, pp. 148–149.
[4] W.B. De Leer, in: J.W. Assink, W.J. Van den Brick (Eds.), Contaminated Soil '85, M. Nijhoff Publishers, Netherlands, 1986, pp. 645–654.
[5] L. Gibbs, M. Punt, in: Tech. Sem. Chem.; Spills, 10th, 1993, pp. 63–84.
[6] R.J. Ayen, C.P. Swanstrom, C.R. Palmer, P.S. Daley, Chim. Ind. 74 (1992) 607.
[7] R.J. Ayen, C.R. Palmer, C.P. Swanstrom, Environ. Sci. Pollut. Control Sci. 6 (1994) 265.
[8] C.P. Varuntanya, M. Hornsky, A. Chernburkar, J.W. Bozzelli, in: International Conference of Physicochemical and Biological Detoxification of Hazardous Waste, 2, 1988, pp. 225–248.
[9] W.L. Troxler, J.J. Cudahy, R.P. Zink, J.J. Yezzi, S.I. Rosenthal, Air and Waste 43 (1993) 1512.
[10] W.L. Troxler, S.K. Goh, L.W.R. Dicks, Air and Waste 43 (1993) 1610.
[11] D. Schneider, M.D. Beckstrom, Environ. Progress 9 (1990) 165.
[12] R.C. Czarneki, J.M. Czarneki, in: P.T. Kostecki, E.J. Calabrese, M. Bonazoutas (Eds.), Hydrocarbon Contaminated Soils, Lewis Publisher, USA, 1992, pp. 695–705.
[13] M.M. McCabe, R. Abrishamian, in: P.T. Kostecki, E.J. Calabrese, M. Bonazoutas (Eds.), Hydrocarbon Contaminated Soils, Lewis Publisher, USA, 1992, pp. 459–468.
[14] J.V. Fletcher, M.D. Deo, F.V. Hanson, Fuel 74 (1995) 311.
[15] E.J. Anthony, F. Preto, in: D.L. Wise, D.J. Trantolo (Eds.), Process Engineering for Pollution Control and Waste Minimization, Marcel Dekker, 1992, pp. 467–485.
[16] M. Hinsenveld, E.R. Soczo, G.J. Van de Leur, C.W. Versluijs, E. Groenedijk, in: F. Arendt, M. Hinsenveld, W.J. Van den Brick (Eds.), Contaminated Soil '90, Kluwer Publishers, Karlsruhe, 1990, pp. 873–882.
[17] G.A. Rogers, Humidity effects on low-temperature thermal desorption of adsorbed volatile organic compounds from soils, PhD Thesis, Illinois Institute of technology, USA, 1989.
[18] J.S. Lighty, E.G. Eddings, E.R. Lingren, X.X. Deng, D.W. Pershing, Combust. Sci. Technol. 74 (1990) 31.
[19] J.S. Lighty, D.W. Pershing, V.A. Cundy, D.L. Linz, Nucl. Chem. Waste Manage. 8 (1988) 225.
[20] J.S. Lighty, G.D. Silcox, D.W. Pershing, V.A. Cundy, D.G. Linz, Environ. Progress 8 (1989) 57.
[21] J.S. Lighty, G.D. Silcox, D.W. Pershing, V.A. Cundy, D.G. Linz, Environ. Sci. Technol. 24 (1990) 750.
[22] V. Bucala, H. Saito, J.B. Howard, W.A. Peters, Environ. Sci. Technol. 28 (1994) 1801.
[23] H.H. Saito, Effects of temperature and heating rate on off-gas composition and pyrene removal from an artificially contaminated soil, PhD Thesis, Dept. of Chemical Engineering, MIT, Cambridge, MA, 1995.
[24] V. Satava, J. Thermal Anal. 5 (1973) 217.

[25] C. Pichon, V. Risoul, G. Trouvé, W.A. Peters, P. Gilot, G. Prado, Thermochim. Acta 306 (1997) 143.
[26] G. Kuhnt, L. Vetter, A. Lattanzio, J. Loens, in: G. Kuhnt, H. Muntau (Eds.), Euro-Soils, Identification, Collection, Treatment, Characterization, Ispra, 1994, pp. 41–58.
[27] G. Kuhnt, W. Koerdel, L. Vetter, N. Bruhn, F. Bo, G. Serrini, M. Bianchi, in: G. Kuhnt, H. Muntau (Eds.), Euro-Soils, Identification, Collection, Treatment, Characterization, Ispra, pp. 59–72.
[28] R. Zaragoza, Application des fluides supercritiques à l'extraction de composés organochlorés dans des matrices de Type Sol, PhD Thesis, INSA, Lyon, France, 1993.
[29] P. Clavelin, Contribution à l'etude de la dépollution des sols par des composés organochlorés: préparation de mélanges témoins, etude comparative de techniques d'extraction, PhD Thesis, INSA, Lyon, France, 1993.
[30] P. Gilot, J.B. Howard, W.A. Peters, Environ. Sci. Technol. 31 (1997) 461.
[31] C. Pichon, Etude des mécanismes fondamentaux intervenant lors de la pyrolyse de sols pollués par des molécules orgniques, PhD Thesis, UHA, Mulhouse, France, 1996.
[32] N. Senesi, in: Molecular and Mechanistic Aspects, NATO ASI, Springer-Verlag, Berlin, G32, 1993, pp. 47–74.
[33] J.J. Pignatello, B. Xing, Environ. Sci. Technol. 30 (1996) 1.
[34] N. Senesi, in: Z. Gerstl, Y. Chen, U. Mingelgrin, B. Yaron (Eds.), Toxic Organic Chemicals in Porous Media, 1989, pp. 37–90.
[35] G. Baranceikova, Z. Gergelova, in: W.J. Van den Brick, R. Bosman, F. Arendt (Eds.), Contaminated Soil '95, Kluwer Academic Publisher, Netherlands, 1995, pp. 357–358.